LETTERS

Resolving photon number states in a superconducting circuit

D. I. Schuster[1]*, A. A. Houck[1]*, J. A. Schreier[1], A. Wallraff[1]†, J. M. Gambetta[1], A. Blais[1]†, L. Frunzio[1], J. Majer[1], B. Johnson[1], M. H. Devoret[1], S. M. Girvin[1] & R. J. Schoelkopf[1]

Electromagnetic signals are always composed of photons, although in the circuit domain those signals are carried as voltages and currents on wires, and the discreteness of the photon's energy is usually not evident. However, by coupling a superconducting quantum bit (qubit) to signals on a microwave transmission line, it is possible to construct an integrated circuit in which the presence or absence of even a single photon can have a dramatic effect. Such a system[1] can be described by circuit quantum electrodynamics (QED)—the circuit equivalent of cavity QED, where photons interact with atoms or quantum dots. Previously, circuit QED devices were shown to reach the resonant strong coupling regime, where a single qubit could absorb and re-emit a single photon many times[2]. Here we report a circuit QED experiment in the strong dispersive limit, a new regime where a single photon has a large effect on the qubit without ever being absorbed. The hallmark of this strong dispersive regime is that the qubit transition energy can be resolved into a separate spectral line for each photon number state of the microwave field. The strength of each line is a measure of the probability of finding the corresponding photon number in the cavity. This effect is used to distinguish between coherent and thermal fields, and could be used to create a photon statistics analyser. As no photons are absorbed by this process, it should be possible to generate non-classical states of light by measurement and perform qubit–photon conditional logic, the basis of a logic bus for a quantum computer.

Cavity QED[3] is a test-bed system for quantum optics[4] that allows investigation of fundamental questions about quantum measurement and decoherence, and enables applications such as squeezed light sources and quantum logic gates. To achieve it, an atom is placed between two mirrors, forming a cavity that confines the electromagnetic field and enhances the atom–photon interaction strength. Cavity QED can be characterized by this interaction strength, g, and the atom cavity detuning, Δ, resulting in several regimes that we represent with the parameter space diagram in Fig. 1. Resonance occurs when the detuning is less than the interaction strength ($\Delta < g$, blue region in Fig. 1), allowing real excitations to be exchanged between the atom and the cavity, resulting in phenomena such as enhanced spontaneous emission into the cavity mode (the Purcell effect[5]). The resonant strong coupling regime of cavity QED is achieved when the coupling rate, g, is larger than the inverse atom transit time through the cavity, $1/T$, and larger than the decay rates of the atom, γ, and the cavity, κ. In this regime, the photon and atom are coherently coupled, and a single photon is periodically absorbed and re-emitted (the vacuum Rabi oscillations) at a rate $2g$. Strong coupling has traditionally been studied in atomic systems using alkali atoms[6], Rydberg atoms[7], or ions[8,9]. More recently, strong coupling with solid state systems has been achieved with superconducting circuits[2,10,11] and approached in semiconducting quantum dots[12,13]. The resonant strong regime of cavity QED is interesting because the joint system becomes anharmonic, allowing experiments in nonlinear optics and quantum information at the single photon level.

In the dispersive (off-resonant) limit, the atom cavity detuning is larger than the coupling, $\Delta \gg g$, and only virtual photon exchange is allowed, keeping the atom and photon largely separable (red and white regions in Fig. 1). The atom (photon) now acquires only a small photonic (atomic) component of magnitude $(g/\Delta)^2$, and an accompanying frequency shift, $2\chi = 2g^2/\Delta$. In this case, the dispersive and rotating wave approximations apply, and the system is described to second order in g/Δ by the quantum version of the a.c. Stark hamiltonian[1]:

$$H = \hbar\omega_r\left(a^\dagger a + 1/2\right) + \hbar\omega_a\sigma_z/2 + \hbar\chi\left(a^\dagger a + 1/2\right)\sigma_z$$

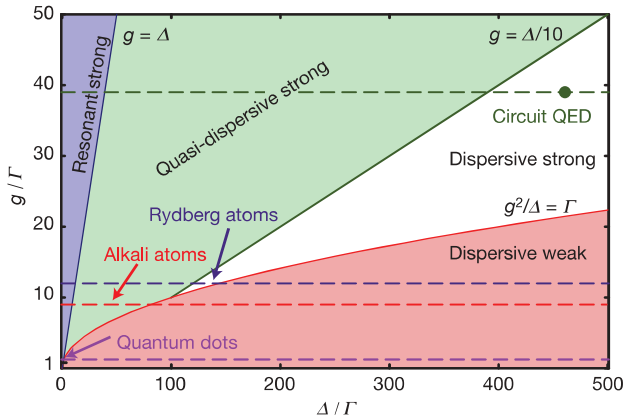

Figure 1 | A parameter space diagram for cavity QED. The space is described by the atom–photon coupling strength, g, and the detuning Δ between the atom and cavity frequencies, normalized to the rates of decay represented by $\Gamma = \max[\gamma, \kappa, 1/T]$. Different cavity QED systems, including Rydberg atoms, alkali atoms, quantum dots, and circuit QED, are represented by dashed horizontal lines. The dark green filled circle represents the parameters used in this work. In the blue region the qubit and cavity are resonant, and undergo vacuum Rabi oscillations. In the red, weak dispersive, region the a.c. Stark shift $g^2/\Delta < \Gamma$ is too small to dispersively resolve individual photons, but a QND measurement of the qubit can still be realized by using many photons. In the white region QND measurements are in principle possible with demolition less than 1%, allowing 100 repeated measurements. In the green region single photon resolution is possible but measurements of either the qubit or cavity occupation cause larger demolition.

[1]Departments of Applied Physics and Physics, Yale University, New Haven, Connecticut 06520, USA. †Present addresses: Department of Physics, ETH Zurich, CH-8093 Zürich, Switzerland (A.W.); Département de Physique et Regroupement Québécois sur les Matériaux de Pointe, Université de Sherbrooke, Sherbrooke, Québec, Canada J1K 2R1 (A.B.). *These authors contributed equally to this work.

The first term describes a single photon mode (a) as a harmonic oscillator of frequency ω_r. The second term describes an atom or qubit, with transition frequency ω_a, as a two-level pseudo-spin (σ_z) system. The third term is a dispersive interaction that can be viewed as either an atom-state-dependent shift of the cavity frequency or a photon-number-dependent light shift (the Stark plus Lamb shifts) of the atom transition frequency. This interaction means that when the atom state is changed, an energy $2\hbar\chi$ is added to or removed from each cavity photon. The form of the interaction is of particular interest because it commutes with the individual atom and photon terms, meaning that it is possible to do a quantum non-demolition[14,15] (QND) measurement of either the atom state by measuring the phase shift of photons in the cavity[16] or photon number using the atomic Stark shift[17,18].

A QND measurement protocol to measure photon number might drive the atom at the Stark shifted atom frequency $\omega_n = \omega_a + 2n\chi$, followed by an independent measurement of the atom state. If the atom is excited, the field must have exactly n photons. Because the photon number is not changed in this process, the QND protocol can be repeated indefinitely. In practice, all measurements have some demolition, which limits the number of repetitions before the measurement changes the measured variable (the number of photons). In our experiment, the cavity transmission is used to measure the atom state, so while the interaction is QND, the detection performed here is not. Any cavity QED experiment that employs a fixed coupling will have demolition arising from the overlap of the atomic and photonic wavefunctions, creating a probability, $(g/\Delta)^2$, that a measurement of photon number will absorb a photon or a measurement of the atomic state will induce a transition, demolishing the measured state. This source of demolition could be minimized by adiabatically changing the coupling strength, as happens in the case of a Rydberg or alkali atom slowly passing through a cavity.

In analogy with the strong resonant case, the strong dispersive limit can be entered when the Stark shift per photon is much larger than the decoherence rates ($2\chi > \gamma, \kappa, 1/T$; the white region in Fig. 1), while the demolition remains small $(g/\Delta)^2 \ll 1$. The small number-dependent frequency shift present in the weak dispersive regime (red region in Fig. 1) becomes so large that each photon number produces a resolvable peak in the atomic transition spectrum, allowing the measurement we report here. It has been proposed that the dispersive photon shift could be used to make a QND measurement of the photon number state of the cavity using Rydberg atoms[19]. Previously attainable interaction strengths required photon number detection experiments to employ absorptive quantum Rabi oscillations in the resonant regime[20], allowing a QND measurement[21] restricted to distinguishing only between zero and one photon. More recently, a non-resonant Rydberg atom experiment entered the strong dispersive limit, measuring the single photon Wigner function with demolition $(g/\Delta)^2 = 6\%$, in principle allowing ~15 repeated measurements[22]. We present here a circuit QED experiment clearly demonstrating the strong dispersive regime, resolving states of up to ten photons, and having demolition $(g/\Delta)^2 < 1\%$, which should allow up to ~100 repeated QND measurements.

In circuit QED[1,16] the 'atom'–photon interaction is implemented by a Cooper pair box (CPB)[23], chosen for its large dipole moment, capacitively coupled to a full-wave one-dimensional transmission line resonator (Fig. 2). The reduced mode volume of a one-dimensional resonator compared with that of a three-dimensional cavity[7] of similar wavelength ($w^2\lambda \approx 10^{-6}\,\mathrm{cm}^3$ versus $\lambda^3 \approx 1\,\mathrm{cm}^3$), where w is the transverse dimension of the resonator, yields 10^6 times larger energy density. This large energy density, together with the large geometric capacitance (dipole moment) of the CPB, yields an interaction strength that is $g/\omega_{a,r} = 2\%$ of the total photon energy. This dimensionless coupling, 10^4 times larger than currently attainable in atomic systems, allows circuit QED to overcome the larger decoherence rates present in the solid-state environment, maintaining $g/\gamma_{eff} = 40$ possible coherent vacuum Rabi oscillations in the strong resonant regime, where $\gamma_{eff} = (\gamma + \kappa)/2$ is the combined photon-qubit decay rate. The equivalent comparison of the dispersive interaction to decoherence examines the Stark shift per photon in relation to the qubit decay, $2\chi/\gamma = 6$, and determines the resolution of photon number peaks. Comparing instead to the cavity lifetime yields an

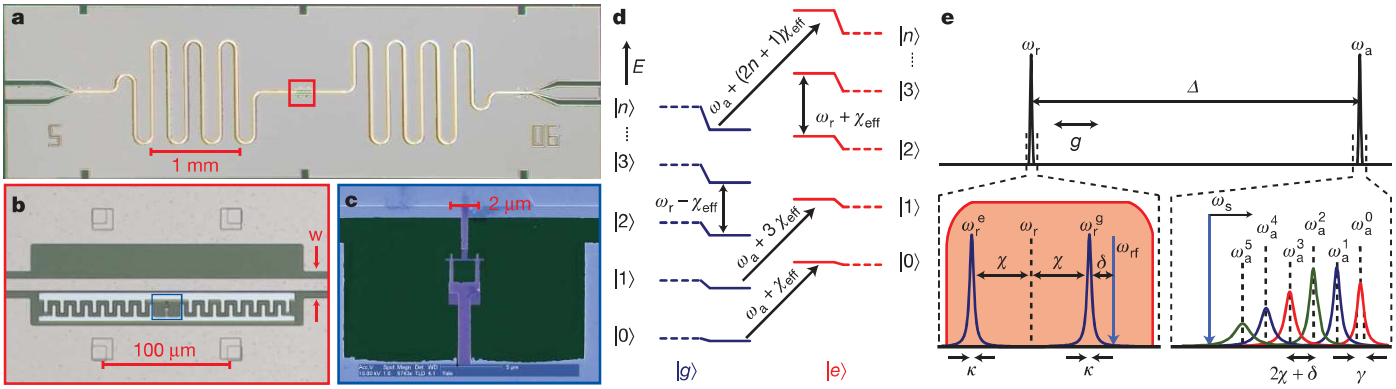

Figure 2 | A Cooper pair box inside a cavity, and spectral features of the circuit QED system. a, An on-chip coplanar waveguide (CPW) cavity with resonant frequency $\omega_r/2\pi = 5.7$ GHz. The area within the red box is shown magnified in **b**. **b**, The Cooper pair box (CPB), placed at a voltage antinode of the CPW (metal is beige, substrate is dark), consists of two superconducting islands (light blue) connected by a pair of Josephson tunnel junctions (purple in **c**). Both the CPB and cavity are made from aluminium. The transition frequency between the lowest two CPB levels is $\omega_a/2\pi \approx \sqrt{8E_JE_C}/h = 6.9$ GHz, where the Josephson energy $E_J/h = 11.5$ GHz and the charging energy $E_C/h = e^2/2C_\Sigma h = 520$ MHz, where C_Σ is the total capacitance between the islands. Both the large dipole coupling, $g/2\pi = 105$ MHz, and the small charging energy are due to the large geometric capacitance of the CPB to the resonator. The anharmonicity is 10%, allowing the first two levels to be addressed uniquely, though higher levels do contribute dispersive shifts, resulting in a negative effective Stark shift per photon, $\chi_{eff}/\pi = -17$ MHz. **d**, Dispersive cavity–qubit energy levels. Each level is labelled by the qubit state, $|g\rangle$ or $|e\rangle$, and photon number $|n\rangle$. Dashed lines are qubit–cavity energy levels with no interaction ($g = 0$), where solid lines show eigenstates dressed by the dispersive interaction. Transitions from $|n\rangle \rightarrow |n+1\rangle$ show the qubit-dependent cavity shift. Transitions at constant photon number from $|g\rangle\,|n\rangle \rightarrow |e\rangle\,|n\rangle$ show a photon-number-dependent frequency shift, $2n\chi_{eff}$. **e**, Cavity–qubit spectral response. To measure the qubit state and populate the cavity, a coherent tone is driven at ω_{rf} (bottom left), which is blue detuned from the cavity by several linewidths, reducing any cavity nonlinearity. Thermal fields are generated with gaussian noise applied in the red envelope, spanning the cavity. The qubit spectrum (bottom right) is detuned from the cavity by $\Delta/2\pi = 1.2\,\mathrm{GHz} \gg g/2\pi$. Information about photon number is measured by monitoring transmission at ω_{rf} while driving the qubit with a spectroscopy tone at ω_s. Each photon shifts the qubit transition by more than a linewidth ($|\chi_{eff}|/2\pi > \gamma/2\pi = 1.9$ MHz, $\kappa/2\pi = 250$ kHz), giving a distinct peak for each photon number state. The maximum number of resolvable peaks is $2|\chi_{eff}|/\kappa$.

estimate of the maximum number of peaks that could possibly be resolved, $2\chi/\kappa = 70$, and determines the contrast of a qubit measurement by the cavity. These values of our parameters place the system well into the strong dispersive regime.

The photon-number-dependent frequency shift of the qubit is detected by performing spectroscopy on the qubit–cavity system (Fig. 2e). The cavity is coherently excited by applying a microwave signal (the cavity tone) at a frequency (ω_{rf}) near the cavity resonance (Fig. 2e). A spectrum is taken by sweeping the frequency (ω_s) of a second microwave signal (the spectroscopy tone), which probes the qubit absorption without significantly populating the resonator as it is detuned by many linewidths ($\omega_s - \omega_r \gg \kappa$). The detection is completed by exploiting the dual nature of the qubit–photon coupling, reusing the cavity photons as a measure of cavity transmission, demonstrated previously[1,2,16,18] to measure the qubit excited state population. The measured transmission amplitude (Figs 3 and 4) is an approximate measure of the actual qubit population, which could in principle be measured independently. For clarity, the transmission amplitude in Figs 3 and 4 is plotted from high to low frequency. In order to reduce nonlinearities in the response, the cavity tone was applied at a small detuning $\delta/2\pi = (\omega_{rf} - \omega_r^g)/2\pi = 2$ MHz from the resonator frequency when the qubit is in the ground state. This also slightly modifies the peak splitting[24] (Fig. 2e).

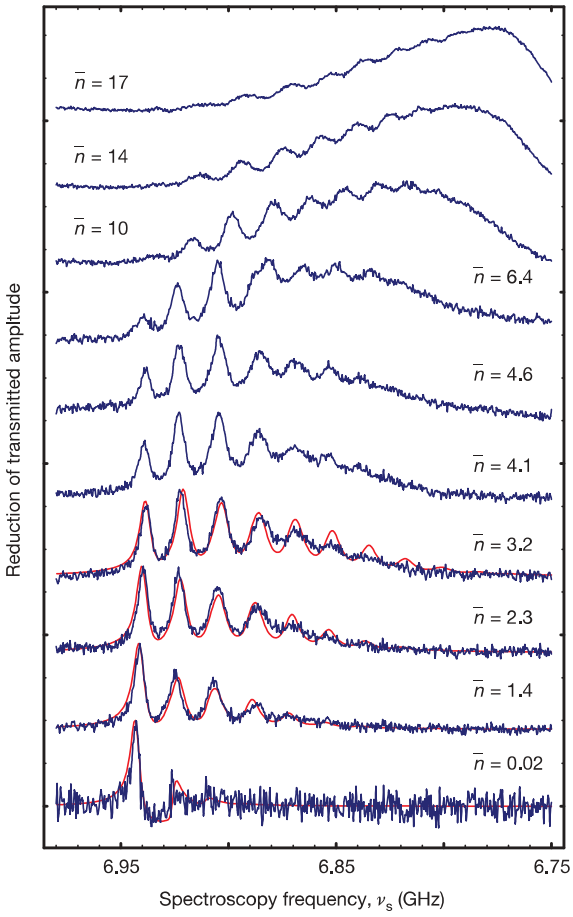

Figure 3 | Direct spectroscopic observation of quantized cavity photon number. Shown are qubit spectra with coherent cavity drive at different average cavity occupations ($\bar{n}$). The spectra have resolved peaks corresponding to each photon number. The peaks are separated by $2|\chi_{eff}|/2\pi = 17$ MHz. Approximately ten peaks are distinguishable. The data (blue) are well described by numerical simulations (red) with all parameters predetermined except for a single frequency offset, overall power scaling, and background thermal photon number ($n_{th} = 0.1$) used for all traces. Computational limitations prevented simulations of photon numbers beyond ~3. At the lowest power nearly all of the weight is in the $|0\rangle$ peak, meaning that the cavity has a background occupation less than ($n_{th} < 0.1$). Peaks broaden as $(n+\bar{n})\kappa/2$ plus some additional contributions due to charge noise. At higher powers the peaks blend together and the envelope approaches a gaussian shape for a coherent state. As $\chi_{eff} < 0$, spectra are displayed from high to low frequency, and also have been normalized and offset for clarity.

The measured spectra reveal the quantized nature of the cavity field, containing a separate peak for each photon number state (Fig. 3)[24,25]. These peaks approximately represent the weight of each Fock state in a coherent field with mean photon number $\bar{n}$, which is varied from zero to 17 photons. At the lowest photon powers, nearly all of the weight is in the first peak, corresponding to no photons in the cavity, and confirming that the background cavity occupancy is $n_{th} < 0.1$. As the input power is increased, more photon number peaks can be resolved and the mean of the distribution shifts proportional to $\bar{n}$. The data agree well with numerical solutions at low powers (solid lines in Fig. 3) to the markovian master equation[4,24] with three damping sources, namely the loss of photons at rate $\kappa/2\pi = 250$ kHz, energy relaxation in the qubit at rate $\gamma/2\pi = 1.8$ MHz and the qubit dephasing rate $\gamma_\phi/2\pi = 1.0$ MHz. However, adequate numerical modelling of this strongly coupled system at higher photon numbers is quite difficult and has not yet been achieved.

In earlier work[17,18] in the weak dispersive limit ($\chi/\gamma < 1$), the measured linewidth resulted from an ensemble of Stark shifts blurring the transition, whereas here in the strong limit ($\chi/\gamma > 1$) each member of the ensemble is individually resolved. In the spectra measured here (Fig. 3), the linewidth of a single peak can be much less than the frequency spread of the ensemble, but changes in photon number during a single measurement can still completely dephase the qubit. Taking this into account yields a predicted photon-number-dependent linewidth, $\gamma_n = \gamma/2 + \gamma_\phi + (\bar{n}+n)\kappa/2$ for the nth peak[24]. The lowest power peak (in the $\bar{n} = 0.02$ trace) corresponds to zero

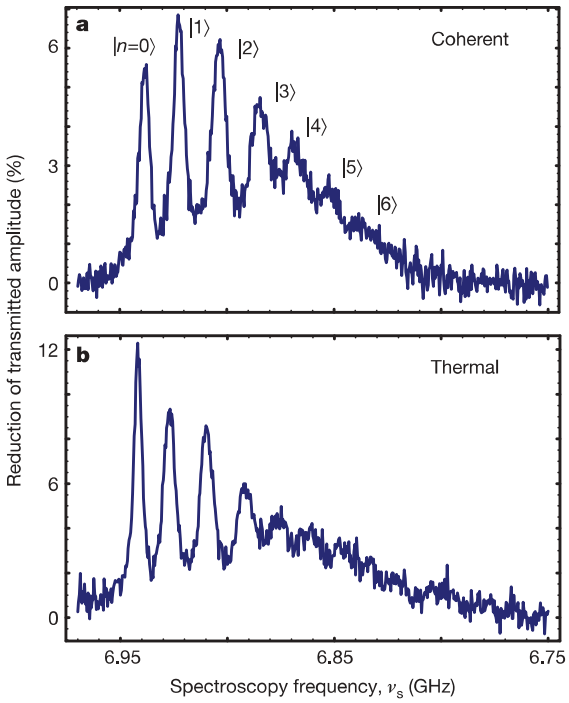

Figure 4 | Qubit spectrum distinguishes between coherent and thermal distributions. **a**, Reduction in transmitted amplitude is plotted as a proxy for qubit absorption for the case of a coherent drive with $\bar{n} = 3$ photons. **b**, Spectrum when cavity is driven with gaussian white noise approximating a thermal state also with $\bar{n} = 3$. The coherent spectrum is clearly non-monotonic and qualitatively consistent with the Poisson distribution, $P(n) = e^{-\bar{n}}\bar{n}^n/n!$, while the thermal spectrum monotonically decreases in a fashion consistent with the Bose–Einstein distribution $P(n) = \bar{n}^n/(\bar{n}+1)^{n+1}$.

photons and measures the unbroadened linewidth, $\gamma_0/2\pi = 1.9$ MHz. When $\bar{n} = 2\chi_{\rm eff}/\kappa$, the peaks should begin to overlap once more, returning the system to the classical field regime. If this effect were the only limitation, we might hope to count as many as 70 photon number peaks before they merge. In practice, the higher number peaks are also more sensitive to charge fluctuations in the Cooper pair box, which limits us to about 10 resolvable photon states in this measurement.

The relative area under each peak in the transmission amplitude (Fig. 4) contains information about the photon statistics of the cavity field. We can compare two cases having the same average cavity occupation ($\bar{n} \approx 3$), but containing either a coherent field (Fig. 4a) or a thermal field (Fig. 4b). To create the thermal field, gaussian noise was added in a wide band around the cavity (red in Fig. 2e). The coherent and thermal states are clearly distinguishable. The weights of the peaks are non-monotonic for a coherent distribution, whereas in the thermal distribution they monotonically decrease[26] for all noise intensities measured. However, for the sample parameters and measurement protocols used here, several effects prevent quantitative extraction of photon number probabilities from the data. First, the inhomogeneous broadening of the higher number peaks due to charge noise prevents independent extraction of their areas. Second, though it has been analytically shown that the qubit absorption spectrum should accurately represent the cavity photon statistics[24], this experiment did not have an independent means to measure the qubit, and there are imperfections in mapping the qubit spectrum onto the cavity transmission. Last, numerical simulations show that spectroscopic driving of the qubit results in complex dynamics that squeezes the cavity photon number, pointing to a path to create exotic states of light, but also partially obscuring the initial photon statistics. The measured data are consistent with numerical predictions that do take into account such squeezing effects (see Fig. 3) for photon numbers ($\bar{n} \leq 3$) that we could simulate. Although these effects are large in the present experiment, an independent measurement of the qubit could be introduced using a second cavity or Josephson-bifurcation amplifier[27], allowing the realization of a quantitative photon statistics analyser. Previous experiments have also measured analogous statistics of other bosonic systems, including phonons in an ion trap[8,9], excitations in a single electron cyclotron oscillator[28], and the number of atoms in a Bose–Einstein condensate passing through a cavity[29].

The results obtained here also suggest a method for photon–qubit conditional logic. The qubit response is now strongly dependent on the number of photons in the cavity. For example, a controlled-not (CNOT) gate between a photon and a qubit could be implemented by applying a π control pulse at the frequency corresponding to one photon in the cavity. This would flip the qubit if there were exactly one photon in the cavity, but do nothing in any other photon number state. Though the resulting qubit state is determined by the presence or absence of a cavity photon, no photons are created or destroyed. The photon can thus be reused to entangle with another distant qubit. A photon-number-based gate is analogous to the phonon common mode coupling used in ion-traps[30], but as the photons travel along transmission lines and not through qubits themselves, many qubits can be placed in a single wavelength, and the photons could be sent to distant qubits, including those in other cavities.

The observation of resolved photon number peaks in the qubit spectrum demonstrates a new regime for cavity QED systems, the strong dispersive limit. Measurement of the spectrum directly reveals the discrete particle nature of the microwave field inside the on-chip cavity, and is used to distinguish field states with different photon statistics. Further exploitation of this exceptionally large vacuum Rabi coupling should enable quantum computing using transmission line cavities as a quantum bus, and allow preparation of quantum states of light for use in quantum communication and nonlinear optics.

Received 20 August; accepted 20 November 2006.

1. Blais, A., Huang, R., Wallraff, A., Girvin, S. & Schoelkopf, R. J. Cavity quantum electrodynamics for superconducting electrical circuits: an architecture for quantum computation. *Phys. Rev. A* **69**, 062320 (2004).
2. Wallraff, A. *et al.* Strong coupling of a single photon to a superconducting qubit using circuit quantum electrodynamics. *Nature* **431**, 162 (2004).
3. Mabuchi, H. & Doherty, A. C. Cavity quantum electrodynamics: Coherence in context. *Science* **298**, 1372–1377 (2002).
4. Walls, D. F. & Milburn, G. J. *Quantum Optics* (Springer, Berlin, 2006).
5. Purcell, E. M. Spontaneous emission probabilities at radio frequencies. *Phys. Rev.* **69**, 681 (1946).
6. Thompson, R. J., Rempe, G. & Kimble, H. J. Observation of normal-mode splitting for an atom in an optical cavity. *Phys. Rev. Lett.* **68**, 1132–1135 (1992).
7. Raimond, J. M., Brune, M. & Haroche, S. Manipulating quantum entanglement with atoms and photons in a cavity. *Rev. Mod. Phys.* **73**, 565–582 (2001).
8. Leibfried, D. *et al.* Experimental determination of the motional quantum state of a trapped atom. *Phys. Rev. Lett.* **77**, 4281–4285 (1996).
9. Leibfried, D. *et al.* Experimental preparation and measurement of quantum states of motion of a trapped atom. *J. Mod. Opt.* **44**, 2485–2505 (1997).
10. Chiorescu, I. *et al.* Coherent dynamics of a flux qubit coupled to a harmonic oscillator. *Nature* **431**, 159–162 (2004).
11. Johansson, J. *et al.* Vacuum Rabi oscillations in a macroscopic superconducting qubit LC oscillator system. *Phys. Rev. Lett.* **96**, 127006 (2006).
12. Reithmaier, J. P. *et al.* Strong coupling in a single quantum dot-semiconductor microcavity system. *Nature* **432**, 197–200 (2004).
13. Yoshie, T. *et al.* Vacuum Rabi splitting with a single quantum dot in a photonic crystal nanocavity. *Nature* **432**, 200–203 (2004).
14. Grangier, P., Levenson, J. A. & Poizat, J. P. Quantum non-demolition measurements in optics. *Nature* **396**, 537–542 (1998).
15. Caves, C. M., Thorne, K. S., Drever, R. W. P., Sandberg, V. D. & Zimmermann, M. On the measurement of a weak classical force coupled to a quantum-mechanical oscillator. *Rev. Mod. Phys.* **52**, 341–392 (1980).
16. Wallraff, A. *et al.* Approaching unit visibility for control of a superconducting qubit with dispersive readout. *Phys. Rev. Lett.* **95**, 060501 (2005).
17. Brune, M. *et al.* From Lamb shift to light shifts: vacuum and subphoton cavity fields measured by atomic phase-sensitive detection. *Phys. Rev. Lett.* **72**, 3339–3342 (1994).
18. Schuster, D. I. *et al.* AC-Stark shift and dephasing of a superconducting qubit strongly coupled to a cavity field. *Phys. Rev. Lett.* **94**, 123602 (2005).
19. Brune, M., Haroche, S., Lefevre, V., Raimond, J. M. & Zagury, N. Quantum nondemolition measurement of small photon numbers by Rydberg-atom phase-sensitive detection. *Phys. Rev. Lett.* **65**, 976–979 (1990).
20. Brune, M. *et al.* Quantum Rabi oscillation: A direct test of field quantization in a cavity. *Phys. Rev. Lett.* **76**, 1800–1803 (1996).
21. Nogues, G. *et al.* Seeing a single photon without destroying it. *Nature* **400**, 239–242 (1999).
22. Bertet, P. *et al.* Direct measurement of the Winger function of a one-photon Fock state in a cavity. *Phys. Rev. Lett.* **89**, 200402 (2002).
23. Bouchiat, V., Vion, D., Joyez, P., Esteve, D. & Devoret, M. H. Quantum coherence with a single Cooper pair. *Phys. Scripta* **T76**, 165–170 (1998).
24. Gambetta, J. *et al.* Qubit-photon interactions in a cavity: Measurement induced dephasing and number splitting. *Phys. Rev. A* **74**, 042318 (2006).
25. Irish, E. K. & Schwab, K. Quantum measurement of a coupled nanomechanical resonator-Cooper pair box system. *Phys. Rev. B* **68**, 155311 (2003).
26. Dykman, M. I. & Krivoglaz, M. A. Profiles of no-phonon lines of impurity centers interacting with local quasilocal vibrations. *Sov. Phys. Solid State* **29**, 210–214 (1987).
27. Siddiqi, I. *et al.* Dispersive measurements of superconducting qubit coherence with a fast latching readout. *Phys. Rev. B* **73**, 054510 (2006).
28. Peil, S. & Gabrielse, G. Observing the quantum limit of an electron cyclotron: QND measurements of quantum jumps between Fock states. *Phys. Rev. Lett.* **83**, 1287–1290 (1999).
29. Ottl, A., Ritter, S., Kohl, M. & Esslinger, T. Correlations and counting statistics of an atom laser. *Phys. Rev. Lett.* **95**, 090404 (2005).
30. Monroe, C., Meekhof, D. M., King, B. E., Itano, W. M. & Wineland, D. J. Demonstration of a fundamental quantum logic gate. *Phys. Rev. Lett.* **75**, 4714–4717 (1995).

Acknowledgements This work was supported in part by the National Security Agency under the Army Research Office, the NSF, the W. M. Keck Foundation and Yale University. A.A.H. acknowledges support from Yale University via a Quantum Information and Mesoscopic Physics Fellowship. A.B. was supported by NSERC, CIAR and FQRNT. Numerical simulations were performed on a RQCHP cluster.

Author Information Reprints and permissions information is available at www.nature.com/reprints. The authors declare no competing financial interests. Correspondence and requests for materials should be addressed to R.J.S. (Robert.Schoelkopf@yale.edu).